Physica C 167 (1990) 579–590
North-Holland

HIGH RESOLUTION NEUTRON POWDER DIFFRACTION INVESTIGATION OF TEMPERATURE AND PRESSURE EFFECTS ON THE STRUCTURE OF THE HIGH-T_c SUPERCONDUCTOR $Y_2Ba_4Cu_7O_{15}$

A.W. HEWAT [a], P. FISCHER [b], E. KALDIS [c], J. KARPINSKI [c], S. RUSIECKI [c] and E. JILEK [c]

[a] *Institut Laue-Langevin, 156X, F-38042 Grenoble, Cedex, France*
[b] *Labor für Neutronenstreuung ETHZ, CH-5232 Villigen PSI, Switzerland*
[c] *Laboratorium für Festkörperphysik ETH, CH-8093 Zürich, Switzerland*

Received 21 February 1990
Revised manuscript received 9 March 1990

We have investigated the effect of temperature and 10 kbar pressure on the structure of the new high-temperature superconductor $Y_2Ba_4Cu_7O_{15}$ ($T_c=68$ K) in an attempt to relate the pressure dependence of T_c in such materials to changes in certain Cu–O distances. The orthorhombic Ammm X-ray model of Bordet et al., with lattice constant $c\approx 50.3$ Å, has been confirmed by our high-resolution neutron powder diffraction measurements. The structure can be described as alternate layers of single CuO-chain ($YBa_2Cu_3O_7$) and double CuO-chain ($YBa_2Cu_4O_8$) blocks. The thermal expansion is anisotropic, with the *b*-axis, parallel to the single and double Cu–O chains, remaining approximately constant for $T<T_c$. As in $YBa_2Cu_4O_8$, Cu–O distances bridging chains and planes, as well as Ba–O distances, are significantly changed by pressure. However, in $Y_2Ba_4Cu_7O_{15}$ these changes are different for the single and double CuO-chain layers. A correlation with the pressure dependence of T_c is proposed.

1. Introduction

We have recently found that significant structural changes are induced in the $T_c=80$ K "124" superconductor $YBa_2Cu_4O_8$ by hydrostatic pressure [1], and we have related these structural changes to the pressure dependence of T_c. A remarkably large, linear increase of T_c occurs in the pressure range 0 to 15 kbar, with $dT_c/dP=0.55$ K/kbar [2]. This increase in T_c is accompanied by a shift of the oxygen atom bridging the double CuO-chains and CuO-planes, towards the latter, implying a transfer of electron holes from the chains to the planes. For the first time, our work showed a direct relation between T_c and a structural change. Similar effects have been observed on oxidising $YBa_2Cu_3O_{6+x}$ [3,4], and on replacing chain Cu^{2+} in $Y_1Ba_2Cu_4O_7$ by Co^{3+} [5,6], but pressure experiments on a well characterised material such as $Y_1Ba_2Cu_4O_8$, which cannot easily lose oxygen [7], are not complicated by changes in stoichiometry.

Bucher et al. [8] have also investigated the pressure dependence of "$YBa_2Cu_{3.5}O_{7\pm x}$". They found a similar strong dependence of T_c on pressure, with $dT_c/dP=0.49$. In contrast to 124, dT_c/dP is not independent of pressure (up to the 15 kbar measured) but the T_c versus P curve shows a saturation point which is dependent on the oxygen content. For $x=0.10$ ($T_c=64$ K) the saturation starts at $P\approx 12$ kbar, and for $x=-0.70$ ($T_c=14.5$ K) it starts already at $P\approx 7$ kbar. The purpose of this investigation is to determine the corresponding changes in the structure of this superconductor with pressure and temperature, and if possible to establish the relation between T_c and bond length changes.

The compound $Y_2Ba_4Cu_7O_{15\pm x}$ (or $YBa_2Cu_{3.5}O_{7\pm x}$), abbreviated 247 or 123.5, has been discovered in 123 melts solidified under high oxygen pressure [9]. Electron diffraction showed an elongated *c*-axis [10]. X-ray diffraction measurements gave the space group Ammm with a lattice constant $c=50.3$ Å for a crystal with $T_c=40$ K [11]. Related electron microscopy and diffraction results have been reported [12,13]. The structure (fig. 1) consists of alternate layers of single CuO-chain ($YBa_2Cu_3O_7$) [14] and double CuO-chain ($YBa_2Cu_4O_8$) [1,15]

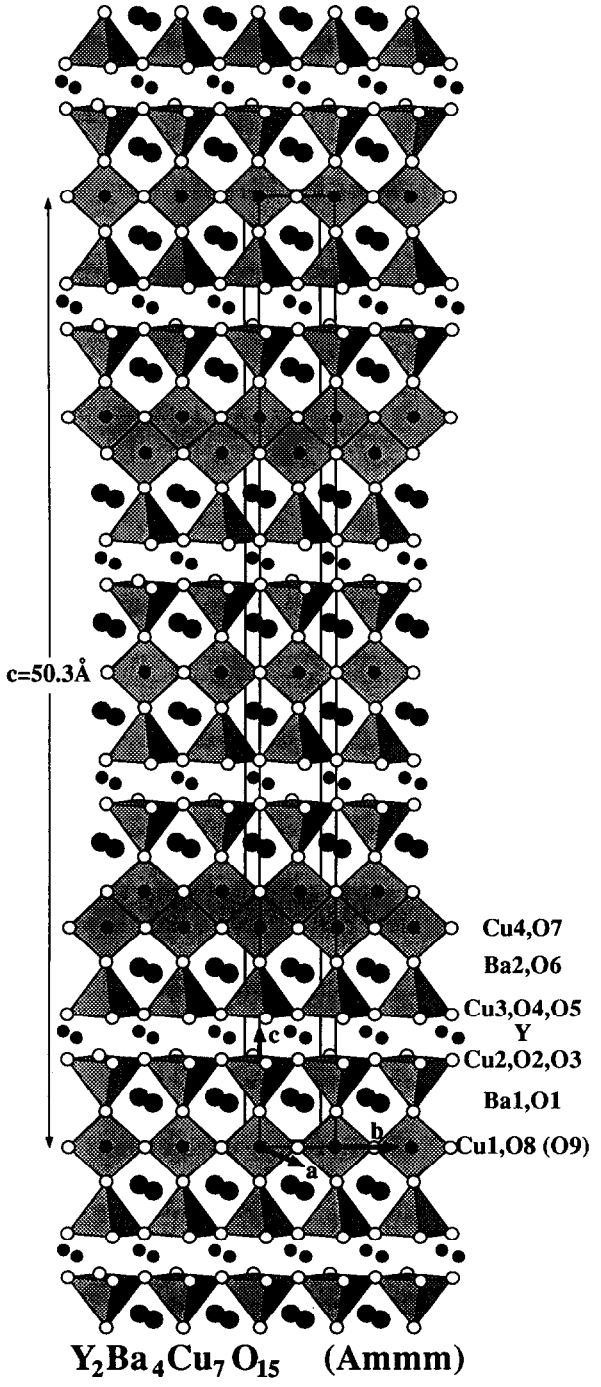

Fig. 1. Crystal structure of $Y_2Ba_4Cu_7O_{15}$ corresponding to space group Ammm. Note the double Cu(4)–O(7) and single Cu(1)–O(8) chains parallel to the *b*-axis, and Cu(2)–O(2,3) and Cu(3)–O(4,5) planes. The minority site O(9) corresponds to single chains disordered perpendicular to the *b*-axis. The small dark circles are Y, and the large Ba.

blocks, and is best written $Y_2Ba_4Cu_7O_{15-x}$. The thermodynamic, structural and physical properties of this new high-T_c superconductor ($0.70 > x > -0.02$) and ($14\ K < T_c < 68\ K$) were recently discussed in detail [18,16]. Clearly, the material used for the X-ray work [11] was oxygen deficient, and curiously, the single CuO-chains appeared to be mainly perpendicular to the double CuO-chains.

For a precise determination of the oxygen distribution, neutron diffraction on fully oxidised samples is needed, and a high resolution powder diffractometer is necessary because of the large lattice dimension ($c \approx 50.3$ Å). In this paper we report on the first neutron diffraction results obtained on stoichiometric $Y_2Ba_4Cu_7O_{15}$ ($T_c = 68$ K) as a function of temperature both at normal pressure and at approximately 10 kbar hydrostatic pressure. A preliminary comparison of temperature and pressure effects on $Y_1Ba_2Cu_xO_y$ compounds was presented at the Paris conference on superconductivity [17].

2. Sample preparation and characterisation

A powder sample of chemical composition $Y_2Ba_4Cu_7O_{14.893}$ with $T = 68$ K was prepared as described in ref. [18] for the neutron diffraction investigations. The oxygen content was determined using a high accuracy volumetric analysis [19]. The X-ray lattice constants for room temperature were measured as $a = 3.8420(6)$ Å, $b = 3.8790(7)$ Å and $c = 50.470(8)$ Å.

3. Neutron diffraction measurements

The "123.5" powder sample enclosed in a cylindrical vanadium container of 8 mm diameter by 40 mm high was first examined on the multidetector powder diffractometer DMC at the Saphir reactor (PSI), using a neutron wavelength of $\lambda = 1.7055$ Å and a scattering angle step of $\delta(2\theta) = 0.05°$. More extensive neutron diffraction measurements were made at the ILL high-flux reactor, on the high-resolution neutron powder diffractometer D2B in the high intensity mode, with an angular step width of $\delta(2\theta) = 0.05°$, and wavelength of $\lambda = 1.5946(3)$ Å. The complete diffraction pattern was measured eight

times at each temperature, and averaged over different detectors to improve statistics and reduce errors.

Measurements were performed in a helium gas atmosphere in the temperature range 5 to 200 K at ambient pressure. The same vanadium container was used for the ambient pressure measurements on D2B and on DMC, but a clamp-type steel pressure cell with Fluorinert pressure transmitting fluid was used for the 10 kbar hydrostatic pressure work as before [1]. The effective sample size was then only 6 mm diameter by 10 mm high; the counting time was therefore tripled, but the count statistics and resulting structure parameters are less good for the high pressure measurements, as indicated by larger error bars. Again the complete pattern was measured eight times at each temperature, and averaged over different detectors.

The DMC measurements were refined, starting from the X-ray parameters [11], with the Wiles and Young program [20] including automatic background fitting. Refinements of all D2B data were made instead with the standard Rietveld program [21] because it was necessary to manually subtract the more complex background from the pressure cell. The D2B refinement procedures were then identical for the ambient pressure and high pressure measurements. Typical observed and calculated neutron diffraction patterns of $Y_2Ba_4Cu_7O_{15}$ are shown in fig. 2 for $T=5$ K (D2B) and 295 K (DMC) at ambient pressure. The sample appears to be essentially single phase and well ordered.

4. Temperature dependence of the $Y_2Ba_4Cu_7O_{15}$ structure

The atomic sites in the space group Ammm are listed in table I. All atoms are in special positions such that the x and y coordinates are fixed by symmetry considerations. With the A-centering condition, which is evident in fig. 1 from the translation of the structure for $z=z+c/2$, there are two formula units $Y_2Ba_4Cu_7O_{15-x}$ in the cell. All atoms are then in 4-fold positions except for the 2-fold sites which constitute the Cu(1)–O(8), O(9) single chains. The occupancy of O(8) would be 2 (and the occupancy of O(9) zero) if the single chains were fully oxidised ($x=0$) and all aligned parallel to the double Cu–O chains.

The structural parameters are summarised in table II (DMC) and table III (D2B) as a function of temperature for ambient pressure. The agreement between the DMC and D2B results is reasonable when account is taken of the uncertainty in the determination of the effective neutron wavelength, which determines the absolute value of the lattice constants; only the error in the *relative* lattice constants is quoted. Because of the higher resolution of D2B at larger scattering angles (even in the high intensity mode) we consider the D2B results of the complex $Y_2Ba_4Cu_7O_{15}$ structure as the most reliable. DMC actually has better resolution at lower scattering angles.

The profile R-factor R_{WP} is lower for the DMC refinement, but this reflects mainly a different definition of R_{WP} in the Wiles and Young program. In the Rietveld program, R-factors are calculated after subtraction of the background, while in the Wiles and Young program (and in some other profile refinement programs) the background is included in the denominator sum, greatly reducing R_{WP}. This is particularly true when the background is relatively important, as for small samples in pressure cells. The Rietveld R-factor, for the D2B data, then appears large by comparison, even though the errors in the structural parameters are generally smaller. The fit to this 247 data is, however, less good than that obtained under similar conditions for 124 [1], presumably because of faults in the stacking of the 123 and 124 blocks; as remarked earlier, the 124 sample appeared particularly good in high resolution electron microscope images.

Isotropic B-factors and full site occupancies were assumed for all atoms, except that the occupancies of the alternative O(8) and O(9) positions in the single chains were refined. Test refinements for other sites revealed no evidence for partial occupancy, so these were fixed at their nominal values. The O(8) and O(9) sites constitute single CuO-chains, respectively parallel and perpendicular to the double CuO-chains in the 124-layer. Since $T_c=68$ K is the most yet observed for $Y_2Ba_4Cu_7O_{15-x}$, it is not surprising that our values of 71% O(8) and 32% O(9), add to nearly 100% single chain oxidation, with the

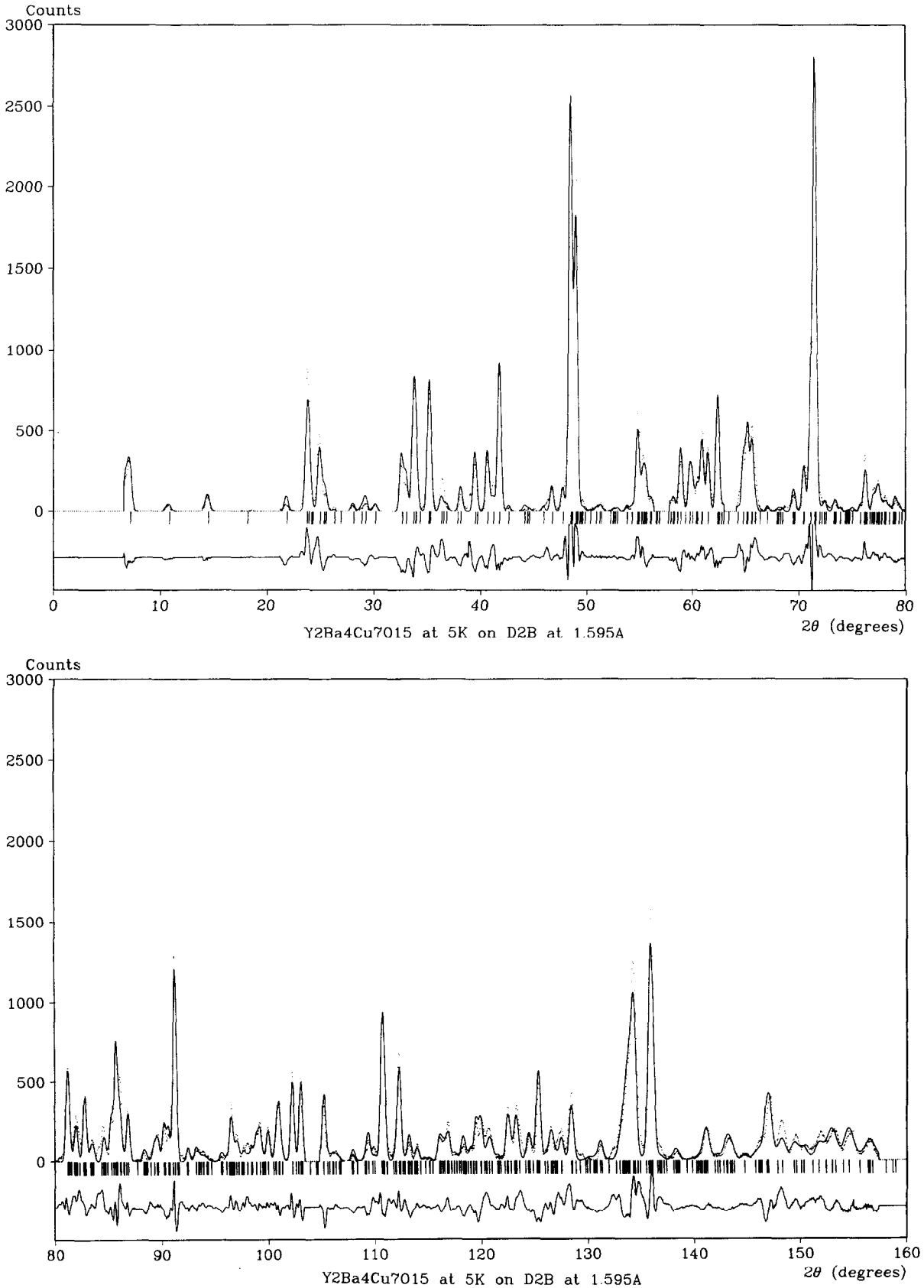

Fig. 2. Observed, calculated and difference neutron diffraction patterns of $Y_2Ba_4Cu_7O_{15}$ at ambient pressure and 5 K on D2B and 300 K on DMC. The neutron wavelength was $\lambda = 1.5946$ Å and 1.7055 Å, respectively. The Bragg peak positions are marked on top by triangles.

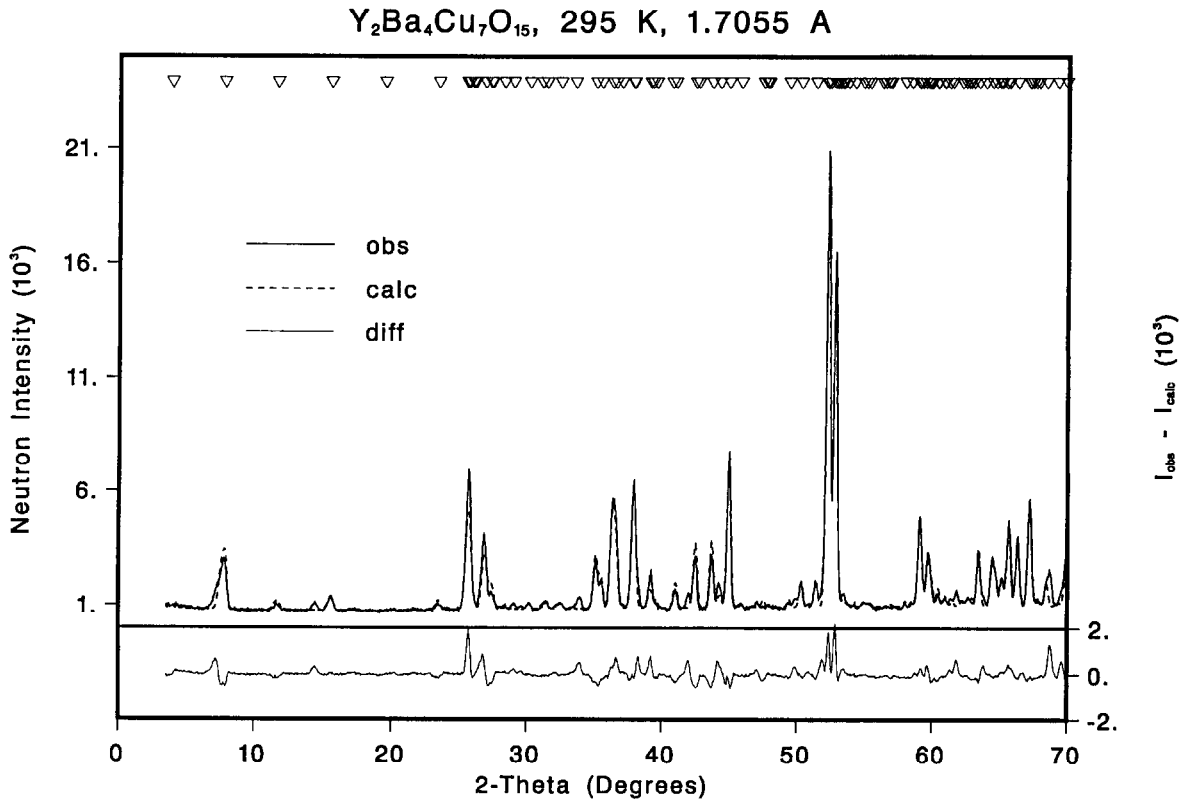

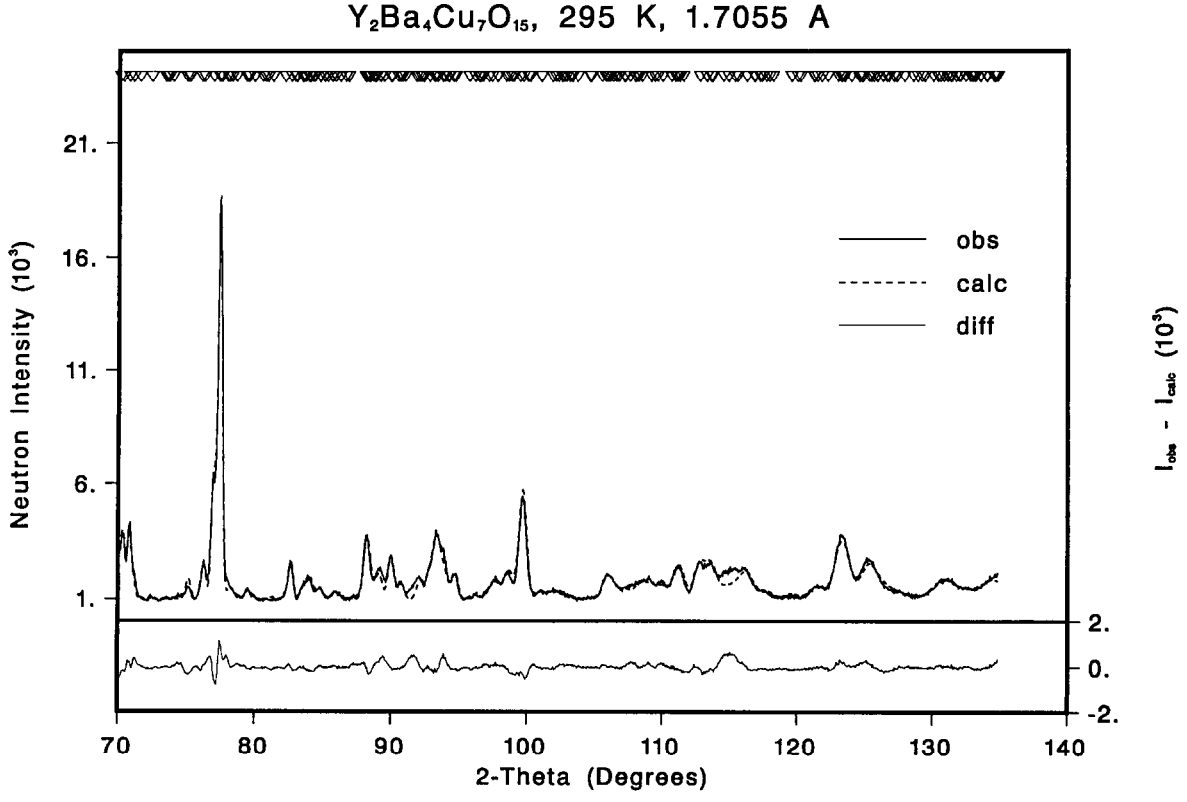

Fig. 2. Continued.

Table I
Occupancies and atom sites (x, y, z) in Ammm for $Y_2Ba_4Cu_7O_{15}$. The 2-fold sites are completed by the A-centering $(x, y+\frac{1}{2}, z+\frac{1}{2})$ and the 4-fold sites also by the inversion centering $(-x, -y, -z)$ and $(-x, -y-\frac{1}{2}, -z-\frac{1}{2})$ equivalent positions. The sites O(8) and O(9) correspond to single CuO-chains respectively parallel and perpendicular to the double CuO-chains, and are only partially occupied ($n<2$ in tables II and III).

Y	4j	$\frac{1}{2}$	$\frac{1}{2}$	Y(z)
Ba(1)	4j	$\frac{1}{2}$	$\frac{1}{2}$	Ba(1)(z)
Ba(2)	4j	$\frac{1}{2}$	$\frac{1}{2}$	Ba(2)(z)
Cu(1)	2a	0	0	0
Cu(2)	4i	0	0	Cu(2)(z)
Cu(3)	4i	0	0	Cu(3)(z)
Cu(4)	4i	0	0	Cu(4)(z)
O(1)	4i	0	0	O(1)(z)
O(2)	4j	$\frac{1}{2}$	0	O(2)(z)
O(3)	4i	0	$\frac{1}{2}$	O(3)(z)
O(4)	4j	$\frac{1}{2}$	0	O(4)(z)
O(5)	4i	0	$\frac{1}{2}$	O(5)(z)
O(6)	4i	0	0	O(6)(z)
O(7)	4i	0	$\frac{1}{2}$	O(7)(z)
O(8)	2b	0	$\frac{1}{2}$	0
O(9)	2d	$\frac{1}{2}$	0	0

single chains mainly aligned along the b-axis (O(8)), parallel to the double chains.

Even so, about one third of the single CuO-chains are misaligned (O(9)) perpendicular to the b-axis in our sample. The earlier X-ray measurements on a single crystal with lower $T_c=40$ K [11] showed only 10% and 20% occupancies of sites O(8) and O(9) respectively. When it was possible to increase the oxygen content of the single chains, T_c was found to increase to 68 K [18]. We are now further investigating the dependence of T_c on the oxygen content of the different sites.

The temperature dependence of this structure is also of particular interest. As in the pure 123- and 124-phases, the thermal expansion is anisotropic (fig. 3). The a- and c-axes as well as the cell volume increase normally with increasing temperature, but the b-axis, parallel to Cu–O chains remains approximately constant for $T<T_c$ in the superconducting state. This is reflected in a change in slope of the orthorhombicity parameter $(b-a)/(b+a)$ close to T_c, again similar to the behaviour of the pure 123- and 124-phases [1,14].

Table II
Structural parameters for $Y_2Ba_4Cu_7O_{15}$ at ambient pressure on DMC ($\lambda=1.7033$ Å). z is the fractional z-ordinate, and B-factor $B=8\pi^2\langle u^2\rangle$ where $\langle u^2\rangle$ is the mean square thermal amplitude in Å^2. See the text for a discussion of the R^{WP}-factor, defined differently in table III.

DMC		22 K	295 K
a	[Å]	3.8347(2)	3.8414(2)
b		3.8725(2)	3.8768(2)
c		50.299(3)	50.470(3)
Y	(z)	0.1147(1)	0.1144(2)
	(B)	0.(3)	0.06(3)
Ba(1)	(z)	0.0425(2)	0.0429(2)
	(B)	0.3(1)	0.6(1)
Ba(2)	(z)	0.1875(2)	0.1879(2)
	(B)	0.3(1)	0.6(1)
Cu(1)	(B)	0.04(5)	0.33(6)
Cu(2)	(z)	0.0819(1)	0.0820(1)
	(B)	0.04(5)	0.33(6)
Cu(3)	(z)	0.1488(1)	0.1486(1)
	(B)	0.04(5)	0.33(6)
Cu(4)	(z)	0.2297(1)	0.2299(1)
	(B)	0.03(5)	0.33(6)
O(1)	(z)	0.0379(2)	0.0374(2)
	(B)	0.32(5)	0.80(6)
O(2)	(z)	0.0852(2)	0.0853(8)
	(B)	0.32(3)	0.80(6)
O(3)	(z)	0.0855(2)	0.0894(2)
	(B)	0.32(5)	0.80(6)
O(4)	(z)	0.1429(2)	0.1433(2)
	(B)	0.32(5)	0.80(6)
O(5)	(z)	0.1442(2)	0.1442(2)
	(B)	0.32(5)	0.80(6)
O(6)	(z)	0.1943(2)	0.1945(2)
	(B)	0.32(5)	0.80(6)
O(7)	(z)	0.2333(2)	0.2331(1)
	(B)	0.32(5)	0.80(6)
O(8)	(B)	0.32(5)	0.80(6)
	(n)	1.74(6)	1.64(6)
O(9)	(B)	0.32(5)	0.80(6)
	(n)	0.48(6)	0.52(6)
R_I		12.04	12.63
R_{WP}		11.39	11.02

As in 124, the rigidity of the b-axis of 247 can be explained by the low compressibility of the double chains, as found by X-ray diffraction in a high pressure diamond anvil apparatus [22]. A structural explanation for this could be the already short Cu(1)–O(1) bond length (1.76 Å at 200 K) as compared for example to $SrCuO_2$ (1.91 Å) [23].

Table III

Structural parameters for $Y_2Ba_4Cu_7O_{15}$ at ambient pressure on D2B. The relative cell dimensions a, b and c are reliable within the quoted standard deviations, but these do not include the uncertainty, due to sample positioning errors, in the effective neutron wavelength 1.5946(3) Å. The sites were all assumed fully occupied, except for O(8) and O(9) where the refined oxygen occupancies, $O(8)(n)+O(9)n \approx 2$ indicate that the single CuO-chains are 70% aligned along the b-axis parallel to the double CuO-chains, and 30% "misaligned" at right angles. See the text and ref. [14] for a discussion of the R_I and R_{WP} factors.

D2B		5 K	35 K	55 K	65 K	75 K	85 K	95 K	105 K	125 K	145 K	165 K	200 K
a	[Å]	3.8388(1)	3.8388(1)	3.8390(1)	3.8390(1)	3.8393(1)	3.8394(1)	3.8396(1)	3.8398(1)	3.8402(1)	3.8407(1)	3.8413(1)	3.8423(1)
b		3.8763(1)	3.8763(1)	3.8763(1)	3.8763(1)	3.8764(1)	3.8764(1)	3.8764(1	3.8765(1)	3.8767(1)	3.8769(1)	3.8772(1)	3.8779(2)
c		50.354(2)	50.354(2)	50.360(2)	50.360(2)	50.367(2)	50.373(2)	50.379(2)	50.386(2)	50.399(2)	50.411(2)	50.431(2)	50.456(2)
Y	(z)	0.1140(1)	0.1140(1)	0.1139(1)	0.1139(1)	0.1141(1)	0.1141(1)	0.1141(1)	0.1141(1)	0.1142(1)	0.1142(1)	0.1142(1)	0.1142(1)
	(B)	0.48(8)	0.48(8)	0.51(8)	0.51(8)	0.50(8)	0.47(8)	0.50(8)	0.52(8)	0.52(8)	0.56(8)	0.57(8)	0.60(8)
Ba(1)	(z)	0.0427(2)	0.0427(2)	0.0427(2)	0.0427(2)	0.0428(2)	0.0429(2)	0.0429(2)	0.0430(2)	0.0430(2)	0.0430(2)	0.0432(2)	0.0433(2)
	(B)	0.37(7)	0.37(7)	0.40(7)	0.40(7)	0.44(7)	0.46(7)	0.45(7)	0.47(7)	0.52(7)	0.53(8)	0.55(8)	0.61(8)
Ba(2)	(z)	0.1883(2)	0.1883(2)	0.1884(2)	0.1884(2)	0.1885(2)	0.1886(2)	0.1887(2)	0.1887(2)	0.1889(2)	0.1888(2)	0.1890(2)	0.1891(2)
	(B)	0.37(7)	0.37(7)	0.40(7)	0.40(7)	0.44(7)	0.46(7)	0.45(7)	0.47(7)	0.52(7)	0.53(8)	0.55(8)	0.61(8)
Cu(1)	(B)	0.43(3)	0.43(3)	0.42(3)	0.42(3)	0.42(3)	0.42(3)	0.42(3)	0.41(3)	0.41(3)	0.41(3)	0.40(3)	0.40(4)
Cu(2)	(z)	0.0818(1)	0.0818(1)	0.0818(1)	0.0818(1)	0.0817(1)	0.0817(1)	0.0818(1)	0.0817(1)	0.0817(1)	0.0817(1)	0.0816(1)	0.0817(1)
	(B)	0.43(3)	0.43(3)	0.42(3)	0.42(3)	0.42(3)	0.42(3)	0.42(3)	0.41(3)	0.41(3)	0.41(3)	0.40(3)	0.40(4)
Cu(3)	(z)	0.1493(1)	0.1493(1)	0.1493(1)	0.1493(1)	0.1491(1)	0.1491(1)	0.1491(1)	0.1491(1)	0.1489(1)	0.1489(1)	0.1489(1)	0.1489(1)
	(B)	0.43(3)	0.43(3)	0.42(3)	0.42(3)	0.42(3)	0.42(3)	0.42(3)	0.41	0.41(3)	0.41(3)	0.40(3)	0.400(4)
Cu(4)	(z)	0.2304(1)	0.2304(1)	0.2304(1)	0.2304(1)	0.2304(1)	0.2305(1)	0.2305(1)	0.2305(1)	0.2304(1)	0.2304(1)	0.2304(1)	0.2304(1)
	(B)	0.43(3)	0.43(3)	0.42(3)	0.42(3)	0.42(3)	0.42(3)	0.42(3)	0.41(3)	0.41(3)	0.41(3)	0.40(3)	0.40(4)
O(1)	(z)	0.0346(2)	0.0346(2)	0.0346(3)	0.0346(2)	0.0347(2)	0.0349(2)	0.0350(2)	0.0349(2)	0.0351(2)	0.0349(2)	0.0348(2)	0.0348(2)
	(B)	0.51(3)	0.51(3)	0.52(3)	0.52(3)	0.52(3)	0.53(3)	0.52(3)	0.53(3)	0.54(3)	0.55(3)	0.55(3)	0.56(3)
O(2)	(z)	0.0865(2)	0.0865(2)	0.0867(2)	0.0867(2)	0.0870(2)	0.0870(2)	0.0871(1)	0.0871(2)	0.0873(1)	0.0874(1)	0.0875(1)	0.0875(1)
	(B)	0.51(3)	0.51(3)	0.52(3)	0.52(3)	0.52(3)	0.53(3)	0.52(3)	0.53(3)	0.54(3)	0.55(3)	0.55(3)	0.56(3)
O(3)	(z)	0.0868(1)	0.0868(1)	0.0866(1)	0.0866(1)	0.0863(1)	0.0862(1)	0.0860(1)	0.0860(1)	0.0859(1)	0.0859(1)	0.0860(1)	0.0860(1)
	(B)	0.51(3)	0.51(3)	0.52(3)	0.52(3)	0.52(3)	0.53(3)	0.52(3)	0.53(3)	0.54(3)	0.55(3)	0.55(3)	0.56(3)
O(4)	(z)	0.1445(2)	0.1445(2)	0.1447(2)	0.1447(2)	0.1449(2)	0.1450(1)	0.1450(1)	0.1450(2)	0.1452(2)	0.1451(2)	0.1452(2)	0.1452(2)
	(B)	0.51(3)	0.51(3)	0.52(3)	0.52(3)	0.52(3)	0.53(3)	0.52(3)	0.53(3)	0.54(3)	0.55(3)	0.55(3)	0.56(3)
O(5)	(z)	0.1437(2)	0.1437(2)	0.1435(2)	0.1435(2)	0.1432(2)	0.1430(2)	0.1429(2)	0.1429(2)	0.1427(2)	0.1428(2)	0.1428(2)	0.1426(2)
	(B)	0.51(3)	0.51(3)	0.52(3)	0.52(3)	0.52(3)	0.53(3)	0.52(3)	0.53(3)	0.54(3)	0.55(3)	0.55(3)	0.56(3)
O(6)	(z)	0.1933(1)	0.1933(1)	0.1933(1)	0.1933(1)	0.1934(1)	0.1934(1)	0.1935(1)	0.1935(1)	0.1936(1)	0.1935(1)	0.1935(1)	0.1935(1)
	(B)	0.51(3)	0.51(3)	0.52(3)	0.52(3)	0.52(3)	0.53(3)	0.52(3)	0.53(3)	0.54(3)	0.55(3)	0.55(3)	0.56(3)
O(7)	(z)	0.232(1)	0.232(1)	0.2321(1)	0.2321(1)	0.2322(1)	0.2323(1)	0.2324(2)	0.2323(2)	0.2325(2)	0.2325(2)	0.2325(2)	0.2326(2)
	(B)	0.51(3)	0.51(3)	0.52(3)	0.52(3)	0.52(3)	0.53(3)	0.52(3)	0.53(3)	0.54(3)	0.55(3)	0.55(3)	0.56(3)
O(8)	(B)	0.51(3)	0.51(3)	0.52(3)	0.52(3)	0.52(3)	0.53(3)	0.52(3)	0.53(3)	0.54(3)	0.55(3)	0.55(3)	0.56(3)
	(n)	1.42(6)	1.42(6)	1.44(6)	1.44(5)	1.44(6)	1.44(6)	1.46(6)	1.46(6)	1.44(6)	1.44(6)	1.38(6)	1.36(6)
O(9)	(B)	0.51(3)	0.51(3)	0.52(3)	0.52(3)	0.52(3)	0.53(3)	0.52(3)	0.53(3)	0.54(3)	0.55(3)	0.55(3)	0.56(3)
	(n)	0.64(6)	0.64(6)	0.64(6)	0.64(6)	0.62(6)	0.64(6)	0.62(6)	0.62(6)	0.62(6)	0.64(6)	0.66(6)	0.66(6)
R_I		15.03	15.03	15.05	15.05	14.74	14.58	14.36	14.82	14.52	14.55	13.86	13.90
R_{WP}		19.71	19.71	19.71	19.71	19.60	19.46	19.48	19.7	19.46	19.52	19.41	19.42

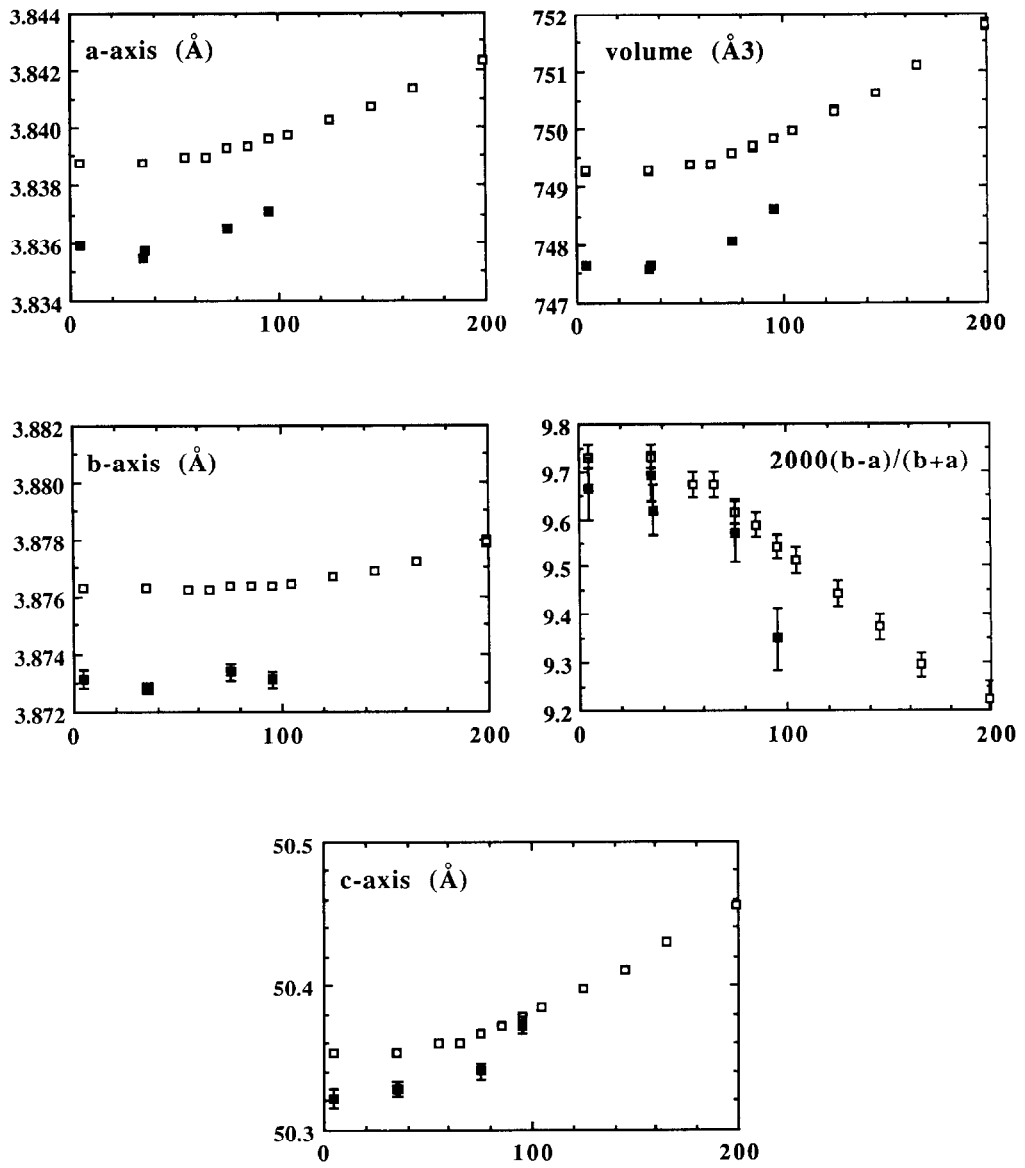

Fig. 3. Temperature dependence of the lattice constants a, b and c in Å, unit cell volume V in Å^3 and orthorhombicity parameter $(b-a)/(b+a)$ for $Y_2Ba_4Cu_7O_{15}$.

5. Pressure effects

The effect of approximately 10 kbar hydrostatic pressure on the structure of $Y_2Ba_4Cu_7O_{15}$ is summarised in table III and illustrated in fig. 3 (solid points). For a discussion of the reasons for the larger errors for the high pressure data compared to the ambient pressure results see ref. [1]. A comparison of the behaviour of 124 under pressure [1] shows an appreciable contraction of not only the b-axis, but also to a lesser extent the a-axis (fig. 3). Since the b-axis contracts a little more than the a-axis, the orthorhombic distortion is slightly reduced. Because of the small uncertainty in the effective neutron wave-

length with and without the pressure cell, our values for the volume contraction are however, less precise than indicated by our error estimates.

6. Bond length changes with temperature and pressure

The variation of the important Cu–O bond lengths with temperature and pressure (solid points) is illustrated in fig. 4. Clearly many bonds, and in particular the in-plane Cu–O lengths, are little changed by temperature or pressure. However, Cu–O distances bridging CuO-chains and CuO-planes are significantly changed at 10 kbar (solid points).

Referring to the structure (fig. 1), the bridging oxygen O(1) in the 123-block moves closer to Cu(2) in the CuO-plane, and away from Cu(1) in the single CuO-chain. In fig. 4, Cu(2)–O(1) is therefore shortened by 4.8‰ while Cu(1)–O(1) is lengthened by up to 2.6‰ when T_c increases at 10 kbar. This is similar to what we have shown for the 124 phase [1]. It is also similar to what happens when $YBa_2Cu_3O_{6+x}$ is oxidised; again this bridging oxygen moves away from the chain toward the plane, a movement that was interpreted by Cava et al. [3,4] as a transfer of charge (electron holes) from the chains to the planes, which was supposed to account for the increase in T_c. A theoretical model has been proposed by Bishop et al. [24] which predicts such charge transfer.

However, the opposite appears to be the case for the 124-block of the 247 structure. In fig. 4, Cu(3)–O(6) lengthens with pressure and Cu(1)–O(1) shortens, so that O(6) moves toward the double CuO-chains. In the pure 124-phase, Kaldis et al. [1] have shown that the bridging oxygen moves instead toward the CuO-plane with pressure, an effect that was again interpreted as charge transfer to the planes, increasing T_c.

We can therefore conclude that although in the pure phase the apical oxygen of the double chains shifts towards the Cu of the planes, in 247 it shifts away from it. Based on refs. [1,3,4,24], it seems reasonable to assume that this reversal decreases the charge on these 124 blocks i.e. on every second copper oxide block (fig. 3).

According to Bucher et al. (fig. 3 in ref. [8]) the saturation of the pressure dependence of T_c starts for $x=0.10$ at approximately 12 kbar. There is an uncertainty of pressures in the present experiment and in ref. [8], as well as lack of investigations about the width of this transition in different samples. It is therefore possible to assume that the negative shift of the apical oxygen in the double chains appears at pressures higher than the onset of saturation in the T_c versus P curve. In this case, the explanation of the form of this curve could be the following [25]. In the linear part, in both 123 and 124 blocks, we suppose that the apical oxygen distance contracts, and that charge transfer takes place from the chains to the planes. Then dT_c/dP would be constant with pressure, and both blocks would contribute to the superconducting coupling. If this working hypothesis is correct, a change from decreasing to increasing Cu(3)–O(6) should occur at $P \approx 7$–12 kbar, corresponding to the saturation of the pressure dependence of T_c.

X-ray and thermogravimetric measurements have shown that T_c decreases rapidly as oxygen is removed from the single chains of the 123 blocks, even though the material still contains complete blocks of the $T_c=80$ K 124 superconductor [16,18]. Changes in the electron hole concentration in the 123-blocks must then produce changes in the adjacent 124-blocks. Superconductivity is apparently more sensitive to changes in the 123-blocks in $Y_2Ba_4Cu_7O_{15}$, and the observed movement at 10 kbar of the bridging oxygen O(1) toward the Cu(2)-plane of the 123 blocks, can again be invoked to account for the increase in T_c with pressure.

There are also significant changes in certain Ba–O distances with pressure. Similar effects were observed with increased pressure in pure $YBa_2Cu_4O_8$ [1], and also with increased oxidation of $YBa_2Cu_3O_{6+x}$ [3,4]. The BaO-plane tends to move as a whole toward the CuO-plane in the 123-block, so that in-plane distances Ba(1)–O(1) (and Ba(2)–O(6)) are not changed with pressure. The remaining Ba–O distances change in accordance with this principle. The movement of the BaO-plane as a whole seems physically reasonable; the resulting changes (and absence of change) in Ba–O distances provide a useful confirmation of the physical reality of the changes in Cu–O distances with pressure.

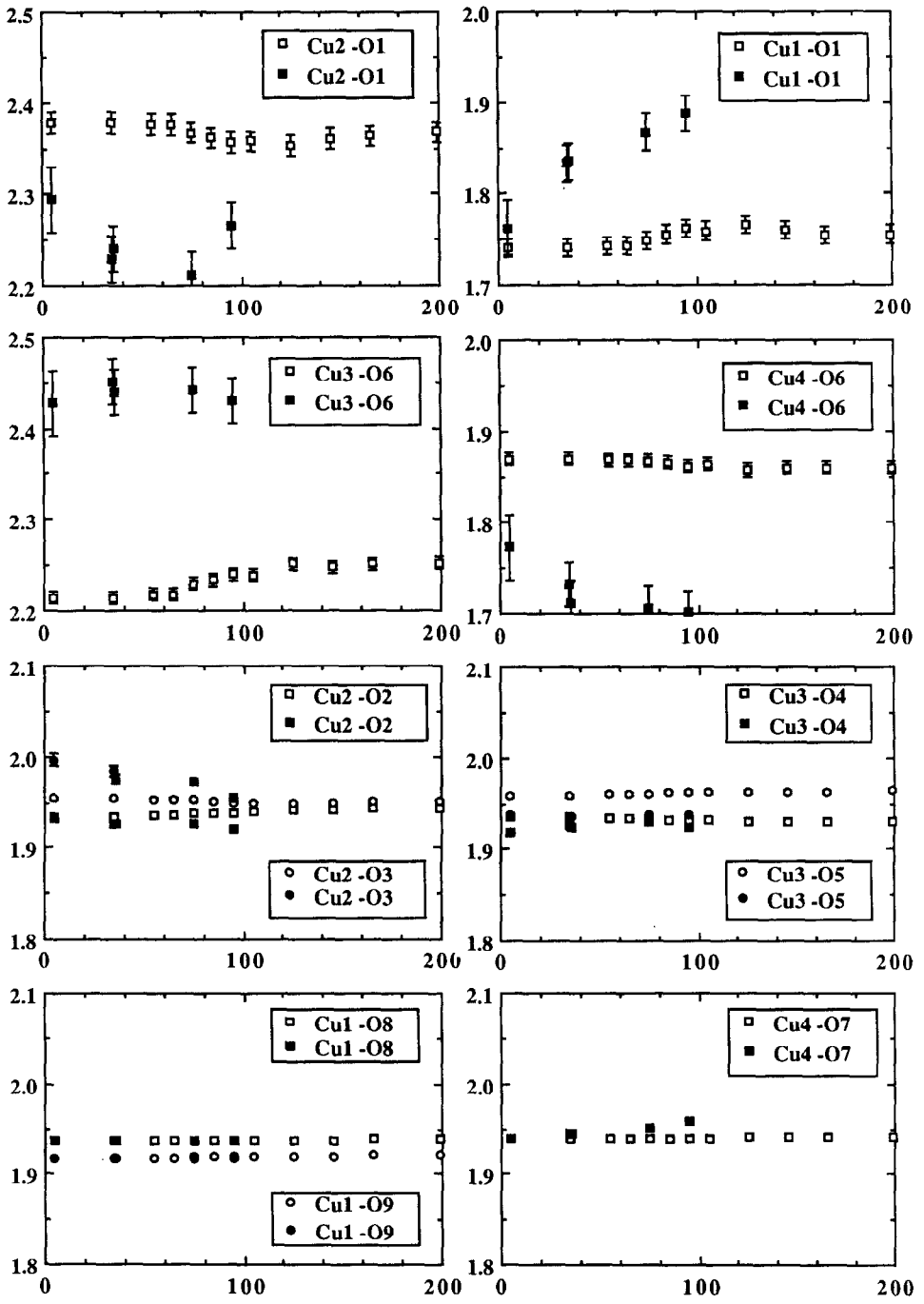

Fig. 4. Temperature variation of the Cu–O bonds (Å) in $Y_2Ba_4Cu_7O_{15}$ at ambient pressure (open symbols)and 10 kbar hydrostatic pressure (solid symbols). The in-plane distances are unchanged, but the distances bridging CuO-chains to planes are strongly affected by pressure. This suggests that charge transfer between chains and planes is associated with the pressure dependence of T_c.

7. Conclusions

These first neutron diffraction results for the new superconductor $Y_2Ba_4Cu_7O_{15}$ confirm the X-ray structure model [11] and yield precise values for the oxygen occupancies for a sample with $T_c = 68$ K, near the maximum T_c observed for this phase. The single CuO-chains are found to be almost fully oxidised, and aligned mainly parallel to the double CuO-chains along the *b*-axis, not oxygen reduced and disordered as for the X-ray sample. The remaining sites are fully occupied, and the complete structure is well ordered despite its complexity.

$Y_2Ba_4Cu_7O_{15}$ expands anisotropicaly with temperature in a similar way to both the pure 123- and 124-phases [1,14]. As in the 124-phase, the *b*-axis remains rather constant up to T_c, while the other axes expand normally. This produces an apparent inflexion in the orthorhombicity of the structure near T_c.

With pressure, significant changes are observed in the Cu–O distances bridging CuO-chains and planes, while distances within the planes are not affected. These changes have again been associated with changes in the distribution of charge within the structure, and this redistribution of charge is probably the reason for the pressure dependence of T_c. Not surprisingly, these effects are more complex in $Y_2Ba_4Cu_7O_{15}$ than in the pure 123- and 124-phases. T_c for this "123.5" phase seems to depend more on the 123-block, since loss of oxygen from the single chains strongly reduces T_c even though the 124-blocks remain intact. The results of this investigation illustrate the model character of this compound for the study of the influence of the CuO_4 chains on superconductivity.

According to Bishop et al. [24], the movement of the bridging or apex oxygen in all of these high-T_c materials has greater significance than a mere static transfer of electron holes to the CuO-planes. They argue that in oxide superconductors, *dynamic* displacement of apex oxygen atoms, in directions perpendicular to the CuO-planes, produces fluctuations in the electron hole density, and that these fluctuations are intimately connected with the superconducting mechanism. Our elastic neutron scattering experiments see only the average structure and displacements, but there is some evidence from high resolution neutron diffraction of "disorder" of the bridging oxygen along the *c*-axis in $YBa_2Cu_3O_7$, in addition to even greater "disorder" within the CuO-chains [26].

Recently, Murayama et al. [27] have found that in the electron-doped superconductor $Nd_{1.85}Ce_{0.15}CuO_{4-\delta}$ with square planar Cu–O coordination, there is no effect of pressure on T_c. In contrast, the hole-doped superconductor $Nd_{1.3}Ce_{0.3}Sr_{0.5}CuO_{4-\delta}$ with pyramidal Cu–O coordination, shows a strong increase in T_c with pressure. This is consistent with our finding that the increase in T_c for the hole-doped materials is characterised by a displacement of the apical (bridging) oxygen toward the CuO-planes. The electron-doped material does not contain apical oxygen.

Acknowledgements

The authors are indebted to the Swiss National Science Foundation and to the ILL Grenoble for financial support.

References

[1] E. Kaldis, P. Fischer, A.W. Hewat, E.A. Hewat, J. Karpinski and S. Rusiecki, Physica C 159 (1989) 668.
[2] B. Bucher, J. Karpinski, E. Kaldis and P. Wachter, Physica C 157 (1989) 478.
[3] R.J. Cava, B. Batlogg, S.A. Sunshine, T. Siegrist, R.M. Fleming, K. Rabe, L.F. Schneemeyer, D.W. Murphy, R.B. van Dover, P.K. Gallagher, S.H. Glarum, S. Nakahara, R.C. Farrow, J.J. Krajewski, S.M. Zahurak, J.V. Waszczak, J.H. Marshall, P. Marsh, L.W. Rupp, W.F. Peck and E.A. Rietman, Physica C 153–155 (1988) 560.
[4] R.J. Cava, A.W. Hewat, E.A. Hewat, B. Batlogg, M. Marezio, K. Rabe, J.J. Krajewski, W.F. Peck Jr. and L.W. Rupp Jr., Physica C 165 (1990) 419.
[5] P.F. Miceli, J.M. Tarascon, L.H. Greene and P. Barboux, Phys. Rev. B 37 (1988) 5932.
[6] R. Sonntag, D. Hohlwein, A. Hoser, W. Prandl, W. Schäfer, R. Kiemel, S. Kemmler-Sack, S. Lösch, M. Schlichenmaier and A.W. Hewat, Physica C 159 (1989) 141.
[7] J. Karpinski, E. Kaldis, E. Jilek, S. Rusiecki and B. Bucher, Nature 336 (1988) 660.
[8] B. Bucher, J. Karpinski, E. Kaldis, S. Rusiecki and P. Wachter, 12th Airapt Conf., Paderborn, 1989, to be published.
[9] J. Karpinski and E. Kaldis, Nature 331 (1988) 242.
[10] J. Karpinski, C. Beeli, E. Kaldis, A. Wisard and E. Jilek, Physica C 153–155 (1988) 830.

[11] P. Bordet, C. Chaillout, J. Chenavas, J.L. Hodeau, M. Marezio, J. Karpinski and E. Kaldis, Nature 334 (1988) 596.
[12] C. Beeli, H.-U. Nissen, Y. Kawamata and P. Stadelmann, Z. Phys. B73 (1988) 313.
[13] C. Chaillout, P. Bordet, J. Chenavas, J.L. Hodeau, M. Marezio, J. Karpinski, E. Kaldis and S. Rusiecki, Solid State Commun. 70 (1989) 275.
[14] J.J. Capponi, C. Chaillout, A.W. Hewat, P. Lejay, M. Marezio, N. Nguyen, B. Raveau, J.L. Soubeyroux, J.L. Tholence and R. Tournier, Europhys. Lett. 3 (1987) 1301.
[15] P. Fischer, J. Karpinski, E. Kaldis, E. Jilek and S. Rusiecki, Solid State Commun. 69 (1989) 531.
[16] E. Kaldis and J. Karpinski, J. Eur. Solid State and Inorg. Chem. (1990) no. 1–2 (in press).
[17] P. Fischer, A.W. Hewat, E. Kaldis, J. Karpinski and S. Rusiecki, Int. Conf. on Superconductivity, Paris, eds. R. Suryanarayanan and A. Niku-Lari (IITT-International, Technology Transfer series, 1989) p. 217.
[18] J. Karpinski, S. Rusiecki, B. Bucher, E. Kaldis and E. Jilek, Physica C 161 (1989) 618.
[19] K. Conder, S. Rusiecki and E. Kaldis, Mater. Res. Bull. 24 (1989) 581.
[20] D.B. Wiles and R.A. Young, J. Appl. Cryst. 14 (1981) 149.
[21] A.W. Hewat, UKAEA Harwell report R 7350 (1973) and ILL report (1974).
[22] H.A. Ludwig, W.H. Fietz, M.R. Dietrich, H. Wühl, J. Karpinski, E. Kaldis and S. Rusiecki (1990) in preparation.
[23] P. Bordet, J.L. Hodeau, R. Argoud, J. Muller, M. Marezio, J.C. Martinez, J.J. Prejean, J. Karpinski, E. Kaldis, S. Rusiecki and B. Bucher, Physica C 162–164 (1989) 524.
[24] A.R. Bishop, R.L. Martin, K.A. Müller and Z. Tesanovic, Z. Phys. B76 (1989) 17.
[25] E. Kaldis et al. (1990) to be published.
[26] M. Francois, A. Junod, K. Yvon, A.W. Hewat, J.J. Capponi, P. Strobel, M. Marezio and P. Fischer, Solid State Commun. 66 (1988) 1117.
[27] C. Murayama, N. Môri, S. Yomo, H. Takagi, S. Uchida and Y. Tokura, Nature 339 (1989) 293.